BMC Rheumatology

RESEARCH

Open Access

Intermittent fasting reduces inflammation and joint damage in a murine model of rheumatoid arthritis: insights from transcriptomic and metagenomic analyses

Rubén Cuevas-Martínez[1], Susana Aideé González-Chávez[1*], Mercedes Bermúdez[2], Joan Sebastian Salas-Leiva[3], Gregorio Vázquez-Olvera[3], Luis Carlos Hinojos-Gallardo[4], Eduardo Chaparro-Barrera[1], César Pacheco-Silva[1], Consuelo Romero-Sánchez[5], Carlos Esteban Villegas-Mercado[2] and César Pacheco-Tena[1*]

Abstract

Background Intermittent fasting (IF) has shown benefits in various pathological conditions. Although its anti-inflammatory potential has been recognized, its effects on the mechanism underlying rheumatoid arthritis (RA) remain insufficiently characterized. This study aimed to investigate the effects of IF in a murine model of RA.

Methods Collagen-induced arthritis (CIA) was developed in sixteen male DBA/1 mice, randomly assigned to two groups, with one undergoing IF every other day for four weeks. The effects of IF on joint inflammation and remodeling were evaluated clinically, histologically, and through tomography. Transcriptomic changes were characterized using expression microarrays, validated by RT-qPCR, and confirmed by immunohistochemistry. Additionally, modifications in gut microbiota were assessed through 16 S sequencing.

Results Mice subjected to IF significantly reduced the incidence and severity of clinical arthritis. Histological and radiographic assessments confirmed a decrease in inflammation and joint damage. Transcriptomic analysis revealed that IF led to the upregulation of 364 genes and the downregulation of 543 genes, with notable reductions in inflammatory signaling pathways associated with RA-related genes, including *Cd72*, *Cd79a*, Ifna, *Il33*, and *Bglap* 2. Notably, *IL33* emerged as a pivotal mediator in the inflammatory processes mitigated by fasting. Key regulators associated with IF effects, such as *CEBPA*, *FOXO1*, *HIF1A*, *PPARG*, and *PPARA*, were identified, indicating a complex interplay between metabolic and inflammatory pathways. Furthermore, differential expression of microRNAs and lncRNAs, including *miR-15b*, *miR-103-2*, *miR-302a*, *miR-6985*, and *miR-* 5624, was observed. Metagenomic

*Correspondence:
Susana Aideé González-Chávez
susana_glezch@hotmail.com
César Pacheco-Tena
dr.cesarpacheco@gmail.com

Full list of author information is available at the end of the article

analysis indicated that IF enhanced the abundance and diversity of the gut microbiome, explicitly promoting anti-inflammatory bacterial populations, notably within the genus *Ruminococcaceae*.

Conclusion Our findings suggest that IF exerts significant anti-inflammatory and immunoregulatory effects in the context of CIA. Given its non-risky nature, further investigation into the potential benefits of IF in patients with RA is warranted.

Clinical trial number Not applicable.

Keywords Arthritis, Collagen-induced arthritis, Fasting, Interleukin-33, Microarray, Pdk4

Background

Rheumatoid arthritis (RA) is an inflammatory autoimmune disease characterized by persistent and destructive synovitis and systemic extraarticular manifestations. This condition imposes a considerable burden on patients, impacting their well-being and functionality while increasing their vulnerability to severe comorbidities that can significantly shorten their life expectancy [1]. Current RA treatments involve pharmacological targeting of known mediators of the inflammatory process. However, despite significant advances, these treatments are only transiently effective for some patients, and treatment refractoriness rates remain substantial [2].

Patients' lifestyles play a significant role in the progression of RA progression and their response to treatment [3]. Dietary modifications, including fasting, have been widely reported to benefit metabolism and extend life expectancy [4]. Intermittent fasting (IF) is a dietary pattern defined by alternating periods of voluntary food and drink abstinence with intervals of regular food intake. Among the most popular and well-studied IF approaches are alternate day fasting (ADF) and the 5:2 method, which involves two days of fasting or severe restriction (75–90% of energy needs) followed by five consecutive days *ad libitum* eating each week [5, 6].

The primary objective of IF is to induce metabolic changes that enhance health outcomes, including improved metabolic flexibility, better weight management, and insulin sensitivity [7, 8]. The IF triggers a range of adaptive responses, including reductions in basal metabolic rates, lipolysis and ketogenesis stimulation, hormone levels modulation, and decreases in oxidative stress and inflammation [9]. The therapeutic benefits of fasting therapy are closely linked to the duration and structure of the fasting periods. While IF can be effective in shorter cycles, longer fasting periods under medical supervision may yield more pronounced health benefits, particularly in metabolic and oncological contexts [10, 11].

The mechanisms by which IF exerts its effects include triggering adaptive autophagy and modifying the intestinal microbiota [12, 13]. Autophagy is regulated by nutrient-sensing signaling pathways, mainly the mammalian target of rapamycin (mTOR) and AMP-activated protein kinase (AMPK) pathways. Fasting activates AMPK and inhibits mTOR, leading to increased mTORC1 activity, which is responsible for insulin and insulin-like growth factor signaling and can suppress autophagy through various mechanisms [14].

On the other hand, numerous studies have shown that IF can modulate the gut microbiome, which influences host physiology, particularly concerning immunity and metabolism [15]. Fasting can rapidly alter the composition and function of the gut microbiome by modulating the abundance of specific microbial species and their individual or collective functions. These IF-induced changes have been shown to increase nutrient and energy utilization, increase the production of short-chain fatty acids (SCFAs), and consequently enhance gut mucosal immune and anti-inflammatory responses [6].

The anti-inflammatory properties of IF have been explored in patients with RA, suggesting its potential as a promising non-pharmacological approach to support disease management [16, 17]. IF significantly reduces RA symptoms and improves disease activity [4, 18, 19]. It has also been suggested that IF may attenuate the inflammatory state by suppressing the expression of pro-inflammatory cytokines, reducing circulating levels of leukocytes [20], and possibly through the production of β-hydroxybutyrate [21]. Nevertheless, the precise mechanisms by which IF exerts this anti-inflammatory effect in RA, including those involved in autophagy pathways and microbiota modulation, are still unknown.

While IF shows therapeutic potential, it also presents documented adverse effects, though studies on long-term impacts remain limited. Commonly reported side effects include dizziness, weakness, and cardiovascular complications associated with hypoglycemia, especially in diabetic individuals [22, 23]. Research on fasting during Ramadan indicates that IF may induce severe hypoglycemic episodes in diabetic patients, particularly those on antidiabetic medication [24–26]. Furthermore, inadequate protein intake during IF can result in muscle atrophy, and some evidence suggests that IF may disrupt the reproductive hormone balance in women [27]. These findings highlight the necessity of careful nutritional planning, warranting an adequate supply of nutrients, to mitigate the associated risks.

Animal research provides valuable insights in describing the molecular aspects of IF under physiological and pathological conditions, including RA. Despite the differences in physiology, feeding behavior, and environmental factors that may influence results, there is a solid basis for comparing IF strategies in mice with those in humans. Animal models of IF have demonstrated significant therapeutic effects on metabolic health, cognitive function, inflammation, and gut microbiota. As in humans, in murine models, IF can be achieved with the most commonly used ADF strategy, with 4 to 16 weeks of intervention periods. This strategy has been shown to prevent weight gain, improve lipid profiles [28], enhance glycemic control [29], and promote an anti-inflammatory response [30, 31]. Concerning the use of RA animal models, the collagen-induced arthritis (CIA) model in DBA/1 mice mimics several features of human disease, including inflammation and joint destruction, and is widely used to study pathogenesis and develop new therapeutic targets [32].

The present study aimed to describe the molecular mechanisms by which ADF exerts its anti-inflammatory effects in a murine model of RA by exploring the joint histopathological and transcriptomic changes and the modulation of the intestinal microbiome.

Methods

Animals and intermittent fasting intervention

A total of sixteen male DBA/1 mice, aged eight weeks (17–20 g), obtained from the animal facility at the Faculty of Medicine and Biomedical Sciences of the University Autonomous of Chihuahua, were included in the experiments. CIA was induced as described below, and before starting the IF intervention, all animals were fed a standard chow diet and water provided *ad libitum* until day 21, when the second collagen injection was administered. At that point, mice were randomly divided into two groups of eight; one group underwent every-other-day IF for four weeks (experimental group), while the other group did not (control group) (Fig. 1).

The sample size was calculated using the formula for comparing two groups based on quantitative data, with a type I error of 5%, statistic power of 80%, and standard deviation (SD) and effect size derived from previous research on the effect of IF in rodent models of inflammation [33], with histological inflammation as the primary outcome.

Mice from both groups were housed in the same building under the same controlled light (12 h light/12 h dark) and temperature conditions (23±2 °C). All mice received water *ad libitum*, while only the control group had food *ad libitum*. Researchers and a veterinarian monitored the mice throughout the experiment. We predetermined that the experiment would be halted if mice exhibited unexpected adverse effects or behavioral changes. No mice were removed from the study; all analyses included eight mice per group. Mice from both groups were euthanized by isoflurane overdose four weeks after the IF intervention in the experimental group, and their hind paws were adequately preserved for transcriptomic and histological analysis.

Collagen-induced arthritis in DBA/1 mice

CIA was induced, as described by Brand et al. [34]. Briefly, under isoflurane anesthesia (Sofloran®, Laboratorios Pisa, Mex), mice were intradermally injected at the base of the tail with a suspension containing 0.1 mg of type II bovine collagen (Sigma Chemicals, St. Louis, MO, USA) emulsified with complete Freund's adjuvant (Sigma Chemicals, St. Louis, MO, USA). A second booster injection was administered on day 21 using Freund's incomplete adjuvant (Sigma Chemicals, St. Louis, MO, USA) with the same amount of collagen (Fig. 1A).

Clinical evaluation of arthritis

The incidence and severity of arthritis were evaluated using a semiquantitative scale: no erythema or swelling (score 0); erythema and mild swelling confined to the tarsals or ankle joint (score 1); erythema and mild swelling extending from the ankle to the tarsals (score 2); erythema and moderate swelling extending from the ankle to metatarsal joints (score 3); and erythema with severe swelling encompassing the ankle, foot, and digits (score 4) [34]. The total score per mouse was calculated by summing the scores for all four limbs. The evaluations were conducted every other day for four weeks following the second collagen injection. Mice were also weighed weekly.

Histological evaluation

After four weeks of IF intervention, the mice were euthanized, and the fore and hind paws of each mouse were dissected ($n=8$). One fore and one hind paw of each mouse were used for histological analysis. After removing the skin and hair, the paws were preserved in 10% formalin phosphate buffer for 48 h and decalcified with 5% nitric acid for 24 h. The tissues were then dehydrated in graded ethanol, embedded in paraffin, sectioned, and stained with hematoxylin-eosin (H&E Merck, Darmstadt, Germany). The histological parameters, including inflammatory infiltrate, synovial hyperplasia, chondral erosion, bone destruction, enthesitis, and cartilage proliferation, were evaluated semi-quantitatively on a scale of 0 (absent) to 3 (severe) for each animal. The mean score for each group was then calculated. Three experienced, blinded operators performed the histological evaluations, which served as the primary outcome measures.

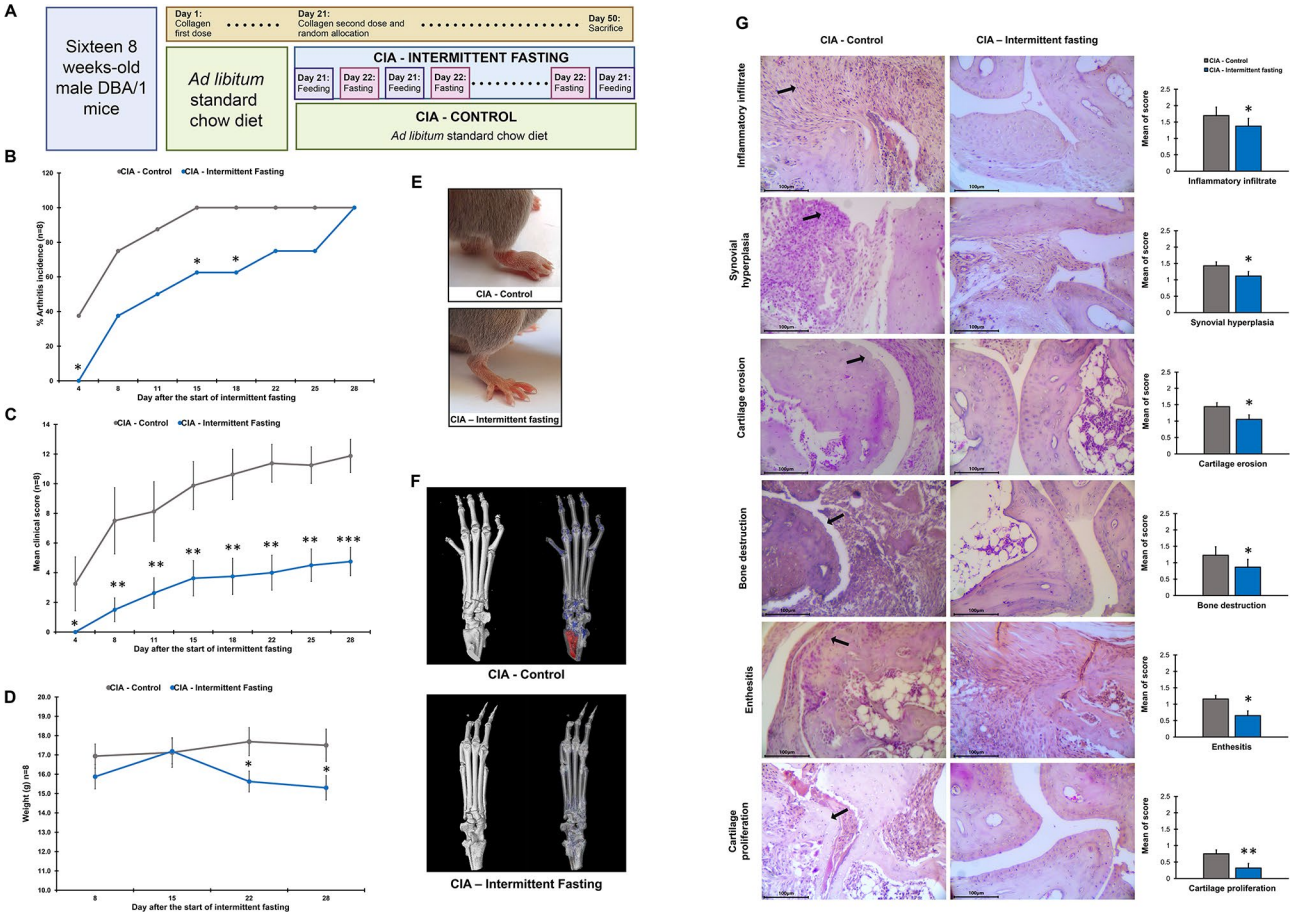

Fig. 1 Clinical and histological anti-inflammatory effects of intermittent fasting in the collagen-induced arthritis model. (**A**) Experimental design for the evaluation of anti-inflammatory effects of IF and the CIA. (**B**) Graph showing the monitoring of the incidence of clinical arthritis throughout the experiment ($n=8$ mice per group). (**C**) Graph showing the evaluation of the effect of IF on arthritis severity throughout the experiment ($n=8$ mice per group). (**D**) Graph showing the monitoring of mouse weight throughout the experiment ($n=8$ mice per group). (**E**) Representative images of clinical severity of CIA mice with and without IF. (**F**) Representative images of the effect of IF on arthritis structural damage through microtomography. (**G**) Representative images and evaluation of the influence of IF on arthritis histological outcomes using H&E staining ($n=8$ mice per group). The arrows indicate the histological area of the finding evaluated in each image. The student t-test was used to determine differences between groups *: $p \leq 0.05$; **: $p \leq 0.01$; ***: $p \leq 0.001$. CIA: Collagen-induced arthritis

Bone density analysis by computational tomography imaging

The formalin-fixed hind paws from the CIA-IF and the CIA-control groups were scanned using a computed tomography (CT) imaging system (Nikon XT H225, Tokyo, Japan) at 100 kV and 98 µA. Each scan consisted of 4,096 projections and 32 frames per projection. The images were processed with VSD Studio Max 3.4 software, and porosity volume was quantified using the Easy-Pore module.

Microarrays hybridization and analysis

Gene expression microarrays were used to compare the IF group (experimental group) with the control group to evaluate the effects of IF on the transcriptome. One hind paw from each mouse was used for this analysis ($n=8$). After dissection, the skin, hair, nails, and muscle were removed from the paw, and the remaining joint structures (bones, joints, and tarsal ligaments) were immediately frozen in liquid nitrogen and pulverized. Total RNA was extracted using the RNeasy® Tissue Mini Kit (QIAGEN, Germantown, MD, USA) according to the manufacturer´s instructions. RNA quality and integrity were assessed using a Qubit 4 fluorometer (ThermoFisher Scientific, Waltham, MS, USA).

Transcript expression analysis of both groups was conducted using Mouse Clariom D® microarrays (GeneChip, Affymetrix, USA). Whole-genome transcriptome hybridization was carried out following the manufacturer's instructions. Briefly, complementary DNA (cDNA) was synthesized and biotin-labeled using the Affymetrix GeneChip WT Pico Kit. After purification, the arrays were processed using the Affymetrix GeneChip™ Hybridization, Wash, and Stain Kit. The arrays were incubated

for 16 h at 45 °C with 60 rpm rotation in a GeneChip 645 hybridization oven. Fluorescence was amplified by adding biotinylated anti-streptavidin and streptavidin-phycoerythrin stain. The fluorescence signal was captured using an Affymetrix GeneChip Scanner 3000 7G plus at a resolution of 3 µm.

Subsequent analysis was conducted with Partek ® Genomic Suite (GS) ® v7.20.0831 software. Samples were normalized using the Robust Multiarray Average (RMA) method, which includes background correction, normalization, and expression value calculation. Differential expression analysis was performed using one-way ANOVA. Differentially expressed genes (DEGs) were selected based on an absolute log2 fold change (log2FC) > 1.5 or < -1.5. The Benjamini-Hochberg false discovery rate [35] was applied to adjust for multiple testing, and genes with an adjusted p-value < 0.05 were deemed significant. DEGs were visualized in the volcano plots and heat maps using the Transcriptome Analysis Console (TAC) Software (Thermo Scientific).

QIAGEN Ingenuity Pathway Analysis (IPA) was employed to assess the biological relevance of DEGs. IPA identified protein-protein interactions and their downstream regulatory effects, selecting the interactions with a minimum confidence score of >0.5) and determining pathway activation or inhibition based on the z-score of each molecule.

The microarray datasets have been registered in the Gene Expression Omnibus (GEO) of the National Center for Biotechnology Information (NCBI) under accession number GSE242986.

Microarray validation by RT-qPCR

RNA quantification was performed using RT-qPCR to validate the following DEGs: Bone gamma-carboxyglutamate protein (*Bglap*)2, interleukin (*Il*)*1* receptor (*r*)*2*, *Il33*, the cluster of differentiation (*Cd*)*36*, and epiregulin (*Ereg*). Primer sets are listed in Supplementary Table 1 (T4 Oligo, Irapuato, GTO, MEX). The reference gene was the ribosomal protein L (*Rpl*)*13* [36]. Total RNA (1 µg) was reverse transcribed into cDNA using the SensiFastTM cDNA Synthesis Kit (Meridian Bioscience, Cincinnati, OH, USA). qPCR was performed in duplicates using the Maxima SYBR Green/ROX (ThermoFisher Scientific, Waltham, MS, USA), with the primer concentrations and aliening temperatures listed in Supplementary Table 1. The specificity of the primers was confirmed via melting curve analysis, and relative quantification (RQ) was determined using the ΔΔCt method ($RQ = 2^{-\Delta\Delta Ct}$).

Immunohistochemistry

Immunohistochemistry (IHC) was performed using specific antibodies against IL-33 (bs-2208R) (Bioss Antibodies MA, USA), osteocalcin (BGLAP) (sc-30045), hypoxia-inducible factor (HIF)-1α (sc-13515), and peroxisome proliferator-activated receptor (PPAR)-γ (sc-7273) (Santa Cruz Biotechnology, CA, USA). Tissue sections were deparaffinized, antigen retrieval was performed with trypsin (T1426-250 mg, SIGMA Life Science, St. Louis, MO, USA), and then tissues were treated with Triton-X100 (Bio-Rad, Hercules, CA, USA). After blocking, the tissues were treated with hydrogen peroxide and incubated overnight with the primary antibody. The corresponding isotype's biotin-streptavidin-conjugated secondary antibodies (Jackson ImmunoResearch Laboratories, Inc, PA, USA) and Pierce® streptavidin horseradish peroxidase-conjugated (Jackson ImmunoResearch Laboratories, Inc, PA, USA) were used for detection, and Diaminobenzidine (DAB) served as the chromogen. Negative controls were established by replacing the primary antibody with PBS. Images were captured using a digital camera (AmScope MU1803, Irvine, CA, USA) and an optical microscope (AxioStar Plus, Carl Zeiss, Berlin, Germany), with at least 20 microscopic fields taken from each slide. The expression of IL-33, BGLAP, HIF-1α, and PPAR-γ was quantified with the ImageJ software and its IHC toolbox. The DAB stain was extracted from each image, and the maximum and mean gray values were obtained. Each image's optical density (OD) was calculated using the formula log10(maximum gray value/mean gray value). The mean OD and SD were then calculated and plotted for each study group.

Metagenomic analysis of feces

Before euthanasia, fecal samples from both groups were collected in sterile microtubes using RNAlater™ (Qiagen, Hilden, Germany) as a preservative. Sample preparation and DNA sequencing were performed at the Microbial Genomics Laboratory (CIAD, Mexico) following standard Illumina amplicon protocols. The V3 region of the 16 S rRNA gene was amplified using universal primers 338 F and 533R. Sequencing was conducted on the Illumina Miniseq platform under standard conditions (300 cycles, 2×150 paired-end reads). Adapters sequences and low-quality bases were removed, and data were processed with Quantitative Insights Into Microbial Ecology (QIIME2) software using the Microbiome Helper [37] and following the Divisive Amplicon Denoising Algorithm (DADA2) pipeline. Sequences were clustered into operational taxonomic units (OTUs) with a 97% identity threshold. OTUs with low confidence (less than 0.1%) were excluded. Diversity indices were calculated using MicrobiomeAnalyst software [38], and data were filtered (IQR = 10%) and normalized using the Cumulative Sum Scale (CSS) [38].

Taxonomic abundances were represented at the genus level using bar plots to illustrate community composition

and structure. Differences between the control and IF-treated groups were assessed by comparing Bray-Curtis distance dissimilarity distances and visualized through non-metric multidimensional scaling (NMDS). Significant differences in beta diversity were determined via permutational multivariate analysis of variance (PERMANOVA) and analysis of similarities (ANOSIM), with significance set at $P \leq 0.05$. Furthermore, T-test/Anova, zero-inflated Gaussian models, and EdgeR analyses were performed on the MicrobiomeAnalyst platform to identify taxa with differential abundance between the control and IF-treated groups, with a false discovery rate (FDR) in $P \leq 0.05$ applied.

Statistical analysis

The statistical analysis was performed using SPSS statics v29 software (Science Inc., Chicago, IL, USA). Measures of central tendency and dispersion were calculated for each variable. The Kolmogorov-Smirnov test was used to assess data normality, and t-tests were employed to compare the effect of IF on clinical, histological, and RNA quantitation data. Differences were considered statistically significant when $P \leq 0.05$.

For bioinformatics analysis, Partek® GS ® 7.20.0831 software was used, applying the Robust Multiarray Averaging (RMA) method for background correction and summarization. This software uses a median polish algorithm, based on log2 transformation, to normalize data for intergroup comparison. Corrected data were analyzed through one-way ANOVA for genes that met the defined fold-change and P-value thresholds. The IPA platform was used to compute the z-score of each gene's *P*- value and log2FC, and its correlation with specific pathways was determined.

Results

Intermittent fasting decreases the incidence and severity of collagen-induced arthritis

The IF effect was clinically and histologically evaluated in DBA/1 mice with CIA. After the second collagen injection on day 21, the mice were randomly divided into two groups; one received IF treatment for four weeks. The incidence of arthritis was monitored over the four-week fasting period (Fig. 1C). Starting on day four after the second collagen injection, 37.5% of mice in the CIA-control group developed arthritis, whereas none of the mice in the IF did. The incidence of arthritis remained lower in the CIA-IF group throughout the experiment until day 28, when all mice in the IF group developed clinical arthritis.

In contrast, the group without IF reached 100% incidence by day 15 of the intervention (Fig. 1C). The CIA-IF group showed lower arthritis severity scores from day four after the second collagen injection (Fig. 1C and E) and a lesser incidence of arthritis. The weight of the mice was monitored throughout the fasting intervention (Fig. 1D). Starting on day 22, the mice subjected to fasting exhibited significant weight loss.

After four weeks of IF, the mice were euthanized, and their fore and hind paws were histologically evaluated through H&E staining. Mice subjected to IF showed significantly reduced scores for inflammatory infiltrates, synovial hyperplasia, and enthesitis. Additionally, tissue remodeling parameters, such as cartilage erosion and bone destruction, were also diminished in the IF group (Fig. 1G). Bone density analysis Through CT imaging further confirmed a decrease in porosity in the hind paws of IF-treated mice (Fig. 1F).

Intermittent fasting down-regulates the inflammatory transcriptomic profile in CIA-mice's joints

The gene expression profiles of both groups were analyzed to understand the biological functions affected by IF. The microarray analysis identified 364 upregulated and 543 downregulated genes (log2FC > 1.5 or <–1.5, adjusted $p < 0.05$) (Fig. 2A), which were validated by RT-qPCR using five DEGs (Fig. 2C). Among the most significantly upregulated genes were *Ereg* (log2FC: 5.57) and pyruvate dehydrogenase kinase (*Pdk*)*4* (log2FC: 4.87), while non-coding RNA (log2FC: -5.16 to -4.16) and nine genes of Major Urinary Proteins (MUP) family (log2FC: -4.08 to -3.68) were highly downregulated. Figure 2B presents a heat map displaying the 50 most significant DEGs based on the p-value.

The IPA regulator effects algorithm identified the key upstream regulators associated with de DEGs (Fig. 2D), including CCAAT enhancer binding protein beta (*Cebpb*), forkhead box protein (*Foxo*)*1*, *Hif1a*, *Pparg*, and *Ppara*. IPA also facilitated functional annotation clustering, classifying DEGs according to their molecular and cellular functions, as detailed in Table 1. Pathways with positive z-scores included *Retinol biosynthesis*, *Macrophage alternative activation*, and *Nicotine degradation II*. Conversely, pathways associated with the inflammatory processes, such as *Systemic Lupus Erythematous (SLE) in the B cell* and the *Osteoarthritis (OA)* pathway, displayed negative z-scores, indicating potential inhibition (Fig. 3). Notably, 17 downregulated genes were linked to the *Altered T cell and B cell signaling in RA*, encompassing *IL33*, *BGLAP* (osteocalcin), *CD79a*, multiple immunoglobulin chains, and T cell receptors.

The predicted consequences of IF on the OA, RA, and SLE pathways are detailed in Supplementary 2. In the OA pathway (Supplementary 2 A), IF inhibited signal molecules, receptors, and transcription factors linked to inflammation and cartilage degradation. In altered T and B cell signaling in RA (Supplementary 2B), IF reduced the expression of *BCR*, *TCR*, and *IL1*, suggesting inhibition of

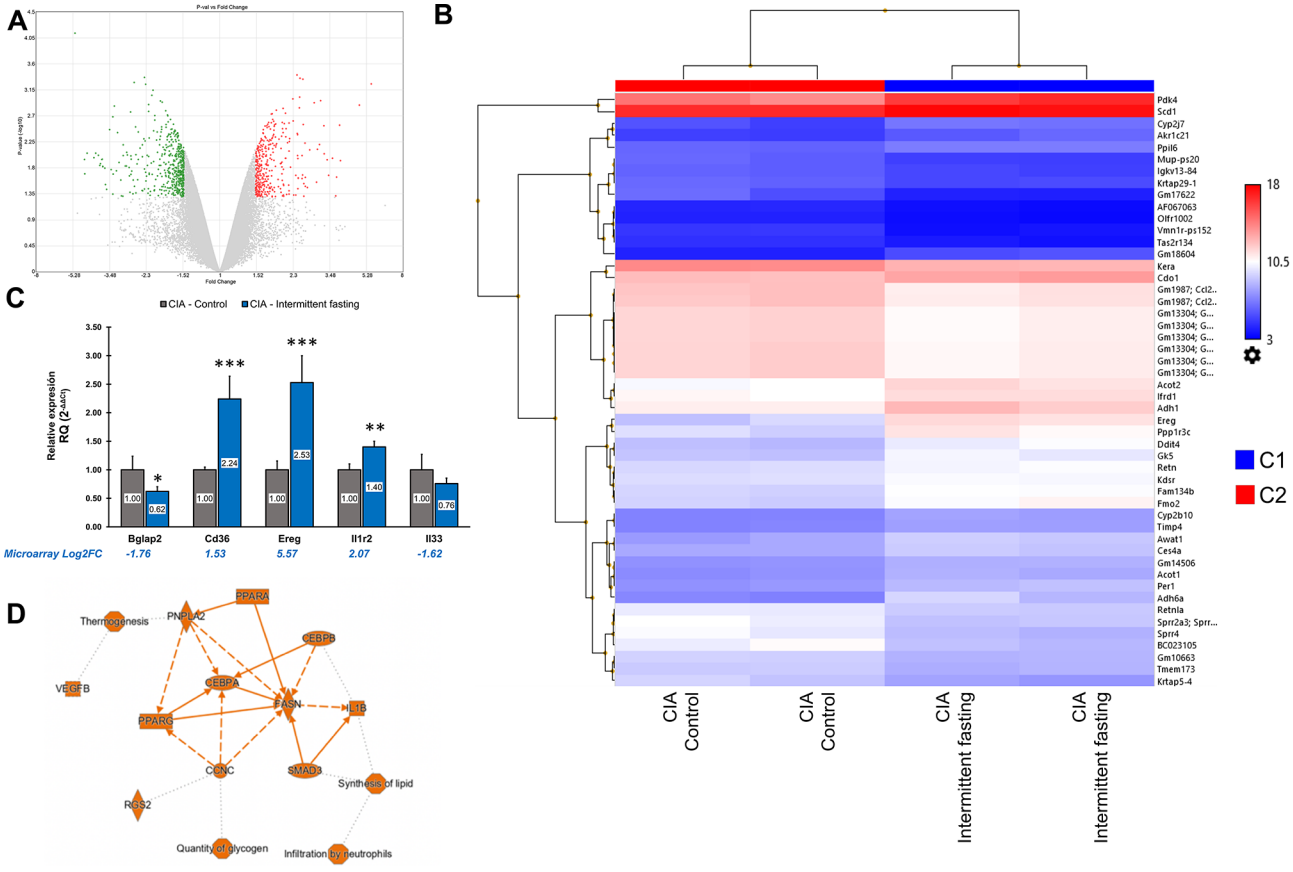

Fig. 2 Dysregulation of transcriptome by intermittent fasting in the collagen-induced arthritis model. (**A**) Volcano plot showing the down- and upregulated gene; the blue zone encloses the genes included in the further analysis ($p \leq 0.01$ and log2FC <-1.5 or >1.5). (**B**) Heat map displaying the 50 most significant DEGs based on the p-value. (**C**) Validation of DNA microarray by relative quantification by RT-qPCR with the ΔΔCT method ($n = 8$ mice per group); the student t-test was used to determine differences between groups *: $p \leq 0.05$; **: $p \leq 0.01$; ***: $p \leq 0.001$. (**D**) Differentially expressed genes were analyzed using the QIAGEN Ingenuity Pathway Analysis (IPA) to assess their biological significance. The analysis and integration of direct protein-protein interactions centered on the functional association and its downstream regulation were obtained, selecting the interactions with minimal confidence (interaction score > 0.5) and considering the pathway's activation or inhibition by the z-score of each molecule. CIA: Collagen-induced arthritis; Bglap2: Bone gamma-carboxyglutamate protein 2; CD36: cluster of differentiation 36; Ereg: Epiregulin; Il1r2: Interleukin 1 receptor 2; Il33: Interleukin 33

Table 1 Effect of intermittent fasting on transcriptome dysregulation in the collagen-induced arthritis model

Effect	Pathway	Genes (Log2FC)
Positive z-score	Retinol Biosynthesis	Ces4a (1.850), Lpl (1.520), Pnpla2 (1.900), Rdh11 (1.550)
	Macrophage Alternative Activation Signaling Pathway	Cd36 (1.530), Il33 (-1.620), Il1r2 (2.070), Irs2 (1.690), Lpl (1.520), Retnla (-1.920), Tsc22d3 (2.230)
	Nicotine Degradation II	Adh7 (2.110), Cyp2b10 (1.830), Fmo2 (2.920) Inmt (1.790)
Negative z-score	Systemic Lupus Erythematosus In B Cell Signaling Pathway	Cd72 (-1.510), Cd79a (-1.840), Ifna13 (-1.550), Ighv5-4 (-2.100), Ighv5-6 (-1.760), Ighv5-15 (-2.100), Ighv8-9 (-1.970), Ighv8-13 (-1.840), Igkv12-89 (-1.900), Igkv13-84 (-1.770), Igkv6-23 (-1.590), Igkv7-33 (-1.840), Igkv8-16 (-1.500), Igkv9-123 (-1.620), Il33 (-1.620), Rasd1 (1.510)
	Osteoarthritis Pathway	Bglap2 (-1.850), Casq1 (-1.710), Ddit4 (3.150), Il1r2 (2.070), Itgb6 (-1.700), Sdc4 (1.720)
No activity available pattern	Altered T Cell and B Cell Signaling in Rheumatoid Arthritis	Cd79a (-1.840), Ighv5-4 (-2.100), Ighv5-6 (-1.760), Ighv5-15 (-2.100), Ighv8-9 (-1.970), Ighv8-13 (-1.840), Igkv12-89 (-1.900), Igkv13-84 (-17-127 (-1.770), Igkv6-23 (-1.590), Igkv7-33 (-1.840), Igkv8-16 (-1.500), Igkv9-123 (-1.620), IL33 (-1.620), Traj29 (-1.600), Trav11d (-1.500), Trav7d-2 (-1.500)
	Phospholipase C Signaling	Cd79a (-1.840), Ighv5-4 (-2.100), Ighv5-15 (-2.100), Ighv8-9 (-1.970), Ighv8-13 (-1.840), Igkv12-89 (-1.900), Igkv13-84 (-17-127 (-1.770), Igkv6-23 (-1.590), Igkv7-33 (-1.840), Igkv8-16 (-1.500), Igkv9-123 (-1.620), Itgb6 (-1.700), Plcd4 (-1.580), Rasd1 (1.510), Rhou (1.750), Traj29 (-1.600), Trav11d (-1.500), Trav7d-2 (-1.500)

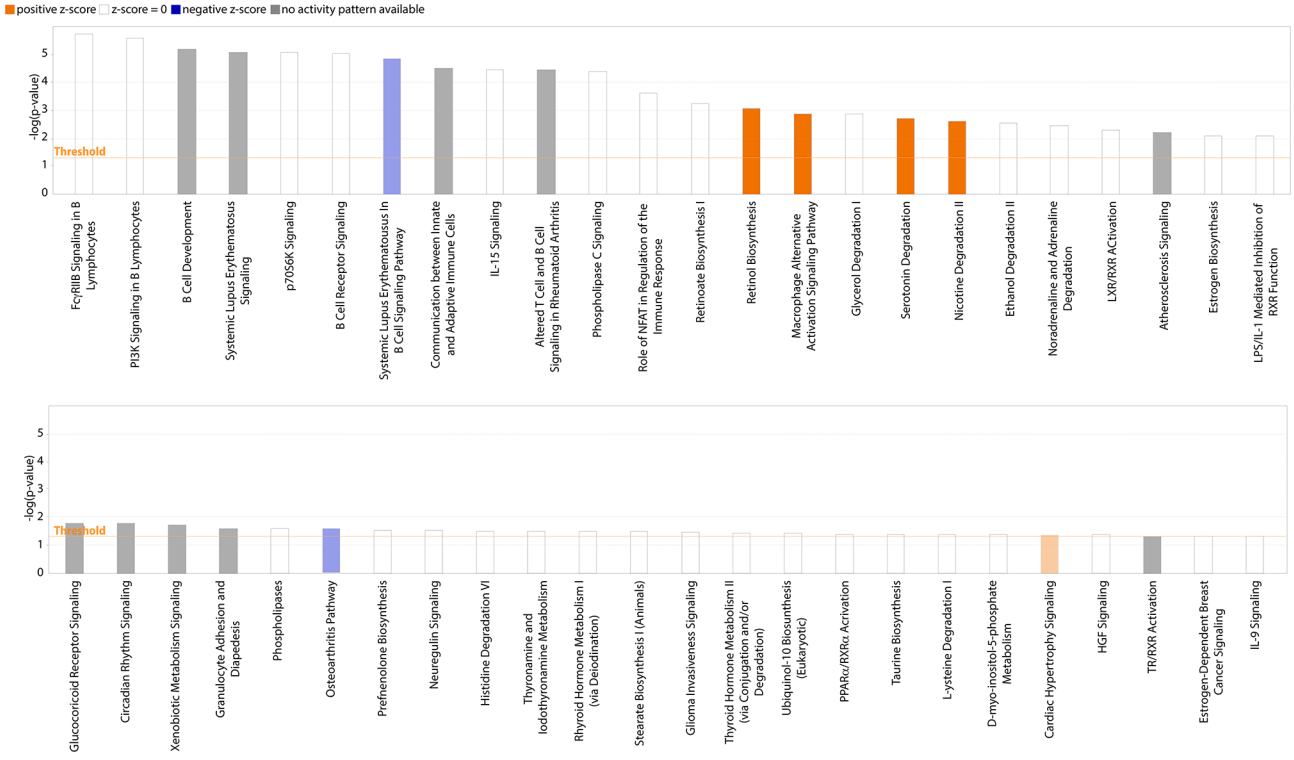

Fig. 3 Diseases and bio-functions related to DEGs by intermittent fasting in the collagen-induced arthritis model. DEGs were classified according to their molecular and cellular function. Genes that met the p-values < 0.01 threshold were associated with biological functions or diseases in the Ingenuity Pathway knowledge. Fischer's exact test was used to calculate the p-value to determine the probability that each biological function/disease assigned to the data set is not due to chance alone

Table 2 Epigenetic effect of intermittent fasting in the collagen-induced arthritis model

Non-coding RNA	Gene symbol (Log2FC)
MicroRNA	Mir15b (2.01), Mir103-2 (1.65), Mir1938 (1.61), Mir7093 (1.55), Mir8106 (1.51), Mir669a-2 (-1.51), Mir883a (-1.55), Mir6336 (-1.59), Mir302a (-1.59), Mir7226 (-1.59), Mir367 (-1.60), Mir1198 (-1.60), Mir6985 (-1.62), Mir759 (-1.74), Mir3963 (-1.78), Mir5624 (-1.84), Mir7055 (-1.87), Mir3964 (-1.96)
lncRNA	2310081O03Rik; RP23-301G2.2 (3.72), Gm19610 (2.05), E230001N04Rik (1.99), Gm17024; RP23-111F7.2 (1.90), Gm16556; RP24-483K3.7 (1.81), LOC100861882 (1.75), LOC100861999 (1.75), LOC100861833 (1.73), Chd3os (1.70), Gm5429 (1.69), LOC100861902 (1.67), 5031426D15Rik (1.66), Gm27177; RP23-103I12.3 (1.58), Gm13748; RP23-45M23.1 (1.58), Gm20022 (1.54), Gm9919 (1.53), Gm26583 (1.52), LOC100862160 (-1.51), 2810471M01Rik (-1.51), 4930588J15Rik (-1.52), Gm13659; RP23-180A8.1 (-1.52), Gm19583 (-1.52), Gm12082; RP23-298H6.1 (-1.55), Gm12478; RP23-390I8.1 (-1.55), Gm26527 (-1.56), Gm27042 (-1.57), LOC100862216 (-1.57), Gm10846 (-1.58), 4930430J02Rik (-1.58), LOC100862098 (-1.60), Gm20456; RP23-242C19.6 (-1.62), Gm19763 (-1.62), Gm15809; RP23-127A20.4 (-1.64), Gm17056; RP24-234D9.2 (-1.65), LOC100862393 (-1.68), Gm26573 (-1.71), Gm26735 (-1.71), Rgs21 (-1.22), 9430019J16Rik (-1.77), LOC100862387 (-2.36)

osteoclast activation and apoptosis. In the SLE pathway (Supplementary 2 C), predictions indicated that signaling in plasmacytoid dendritic cells and B cells decreased the expression of *CCND1*, *CCND2*, *CCND3*, *MYC*, *BCL2*, *MCL*, and *ISG*, leading to reduced germinal center formation, B cell proliferation, and severe SLE.

DEGs were also associated with cellular functions and diseases, represented in heat maps (Supplementary 3). Molecular transport, small molecule biochemistry, lipid metabolism, carbohydrate metabolism, and cell development were enhanced by IF (orange boxes). Conversely, cell signaling, protein synthesis, inflammatory response, and various metabolic and endocrine disorders were reduced (pink box) (Supplementary 3 A). Further exploration of the inflammatory response (Supplementary 3B) revealed that IF decreased inflammation and immune response, predicting a suppression of the experimentally induced arthritis (pink box in Supplementary 3B).

Intermittent fasting also modified the expression of 66 genes classified as miRNA precursors or non-coding RNAs, including miRNAs (5 upregulated, 8 downregulated) and lncRNAs (4 upregulated, 5 downregulated) (Table 2). Some miRNAs, such as *miR-15b*, *miR-103-2*, *miR-302a*, *miR-6985*, and *miR-5624*, have been previously linked to joint inflammation [39–44].

Finally, IHC confirmed significantly lower *IL-33* expression in IF-treated mice than those fed *ad libitum* (Fig. 4A), with *IL-33* predominantly found in synovial membrane structures and expressed in the nucleus and cytosol. In contrast, *BGLAP* (Fig. 4B) showed a reduction in microarray and RT-qPCR analyses, but IHC did not reveal significant differences, suggesting post-transcriptional regulation. The predicted central mediators of IF's anti-inflammatory effects in CIA, *HIF-1α* (Fig. 4C), decreased in IF-treated mice, while *PPAR-γ* (Fig. 4D) was upregulated. *HIF-1α* was mainly expressed in synovial membranes and chondrocytes, whereas *PPAR* showed cytoplasmic expression in the synovial membrane and bone marrow, where adipose tissue is most abundant.

Modulation of the gut microbiome by intermittent fasting as a possible anti-inflammatory mechanism

Intermittent fasting altered the gut microbiota in mice, as depicted in Fig. 5, which shows the bioinformatic analysis of metagenomic sequencing data. The gut microbiome of

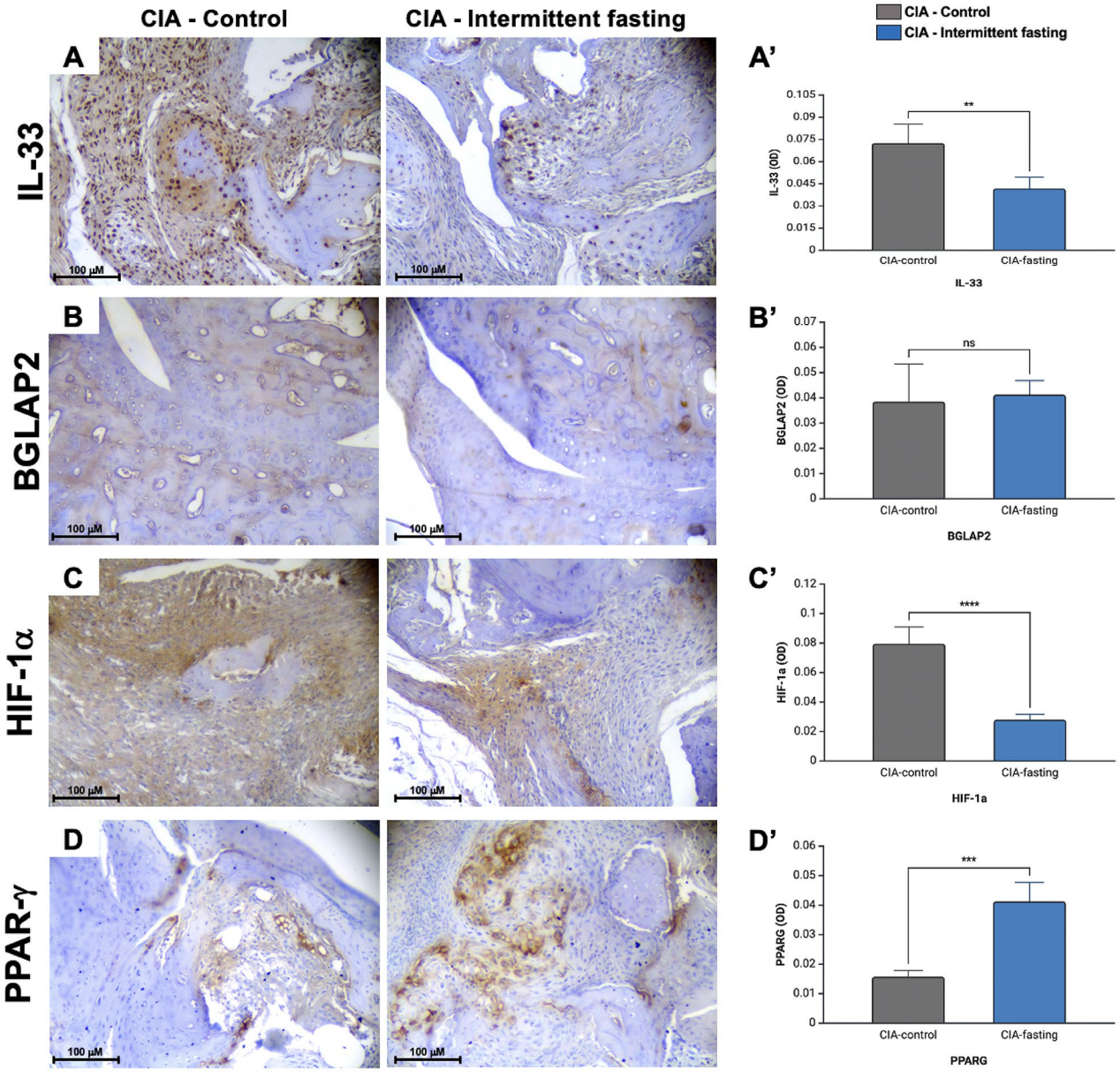

Fig. 4 Effect of Intermittent Fasting on the expression of IL-33, BGLAP, HIF-1α, and PPAR-γ in the hind paws' joints of collagen-induces arthritis mice. Representative images of the expression of IL-33 (**A**), BGLAP (**B**), HIF-1α (**C**), and PPAR-γ (**D**) in tarsal joints of DBA/1 mice non-treated (left) and treated with IF (right). The images were acquired with 10X and 40X amplification. Optical Density (OD) mean and standard error (SE) are shown in graphics (**A**', **B**', **C**,' and **D**'). The student's t-test was used to determine statistically significant differences. *: $p \leq 0.05$, ** $p \leq 0.01$. $n = 8$ mice per group

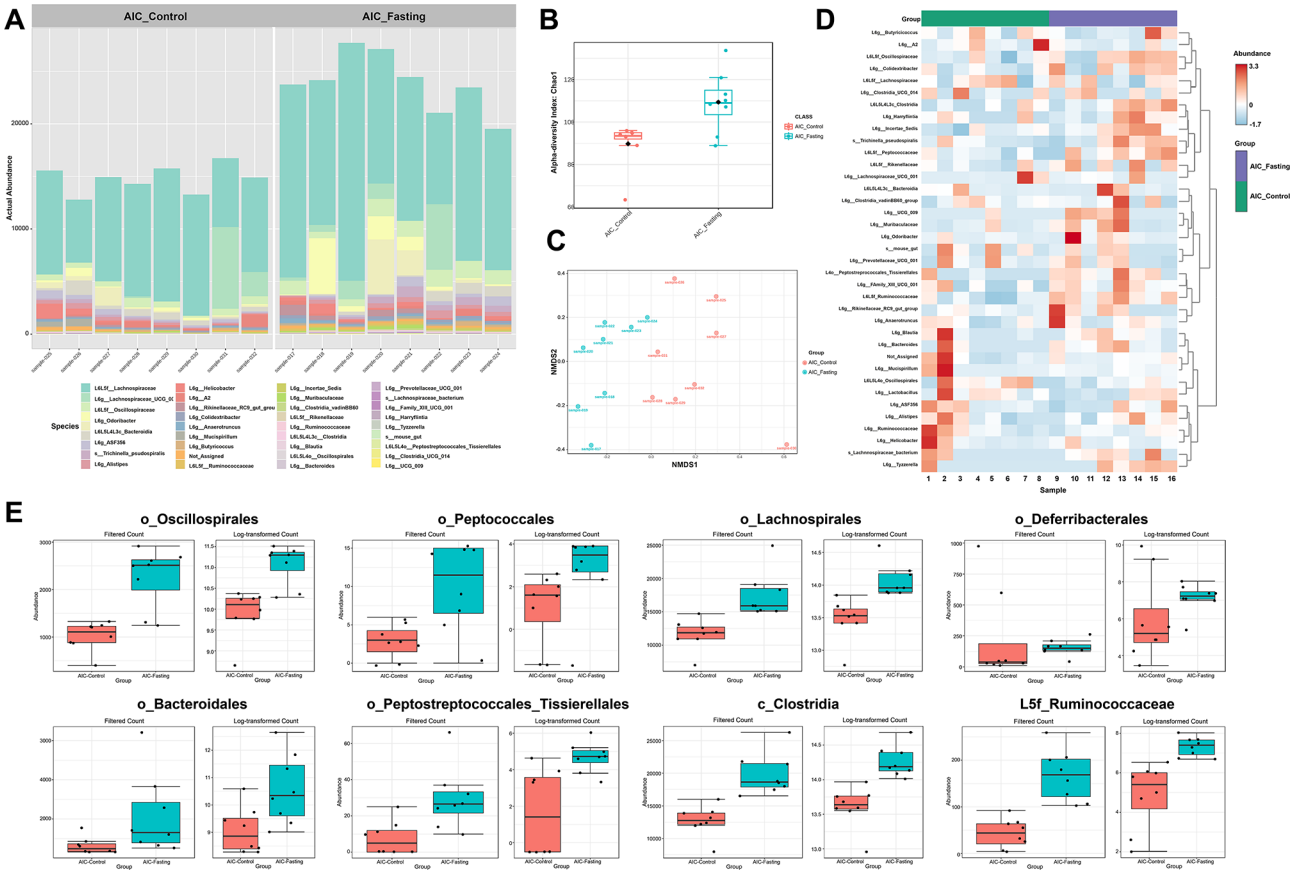

Fig. 5 Modification of the gut microbiome induced by intermittent fasting in the collagen-induced arthritis model. (**A**) Composition and structure of the microbial community of feces from control and IF mice. (**B**) Alpha diversity index (Chao-1); (**C**) Beta diversity at the OTU level is spatially represented by a non-multidimensional scaling analysis (NMDS) using Bray Curtis dissimilarity distances. (**D**) Heat map of the abundance of bacterial species in the two study groups. (**E**) Graphs from the univariate analysis of those classes, orders, and genera different in the group treated with IF ($p < 0.01$ and FDR < 0.05)

IF-treated mice was more abundant and diverse than the control group (Fig. 5A). The Chao1 index revealed significantly higher alpha diversity in the IF group ($p=0.008$) (Fig. 5B), while Fig. 5C illustrates the difference in beta diversity between the study groups.

The heat map (Fig. 5D) highlights the differential abundance of various bacterial species between the groups. Univariate analysis indicated that the orders *Oscillospirales* ($p=0.0004$, FDR=0.003), *Peptococcales* ($p=0.0006$, FDR=0.003), *Lachnospirales* ($p=0.0044$, FDR=0.013), *Deferribacterales* ($p=0.0055$, FDR=0.013), *Bacteroidales* ($p=0.0065$, FDR=0.013), and *Peptostreptococcales Tissierallales* ($p=0.0066$, FDR=0.013) were significantly more abundant in IF-treated mice. At the genus level, *L5f Ruminococcaceae* was more prevalent in the IF group (Fig. 5E).

Discussion

IF has demonstrated beneficial effects in reducing RA symptoms [20, 21]; however, the cellular mechanisms underlying this clinical improvement remain unclear. This study reveals the anti-inflammatory effects of IF in a murine model of RA at the transcriptomic, histological, clinical, and tomographic levels through the deregulation of coding and non-coding genes. This deregulation results in reduced inflammation and greater preservation of joint structure. Additionally, metagenomic sequencing suggests that IF alters the abundance and diversity of gut microbiota, increasing bacteria associated with anti-inflammatory effects, which may be linked to the observed joint-level outcomes.

The molecular mechanisms underlying the anti-inflammatory effects of IF have been previously demonstrated in animal models of non-articular inflammation [45, 46]; however, to our knowledge, this is the first study to show the transcriptomic and metagenomic anti-inflammatory effects of IF in an RA model. Our results indicate that the integration of DEGs within the OA, SLE, and RA pathways predicts a reduction in the inflammatory process and joint damage, as confirmed by our clinical, histological, and radiographic analyses. OA and RA share common osteochondral destruction driven by inflammation, where close interaction exists between osseous tissues and immune cells through inflammatory cytokines [47].

In our study, genes involved in the OA signaling pathway, which overlap with the pathogenesis of CIA and RA, were modulated by IF, including *Bglap* [48] and Syndecan-4 (*Sdc4*) [49]. Additionally, RA and SLE share interconnected etiologies and pathogenesis, with gene signatures involved in innate and adaptive immune responses, bone development, and growth [50].

Our bioinformatic analysis predicted that genes such as *CEBPA*, *FOXO1*, *HIF1A*, *PPARG*, and *PPARA* are key regulators in the effects of IF on CIA. Moreover, our IHC analysis confirmed the downregulation of *HIF-1α* and the upregulation of *PPAR-γ* proteins in the tarsal joints of IF-treated mice. Current evidence links these regulators to RA pathogenesis, and numerous experimental treatments exert anti-inflammatory effects through them [51–54], suggesting that the molecular mechanisms triggered by IF may overlap with those of current targets.

The genes most strongly deregulated by IF included *Ereg* (log2FC: 5.57), *Pdk4* (log2FC: 4.87), and *MUPs* (log2FC: -4.08 to -3.68). *Ereg* has been associated with inflammation and fibrosis and is upregulated in inflammatory diseases such as RA, where fibroblast-like synoviocytes produce it. Although it may seem paradoxical that IF, which exerts anti-inflammatory effects, upregulated this proinflammatory mediator, it is known that IF stimulates glucagon secretion. While the fasting-glucagon-epiregulin relationship has not been thoroughly described, glucagon-like peptide-2 upregulates *Ereg* [55, 56], leading us to hypothesize that the induction of *Ereg* by IF remains within physiological margins.

The upregulated gene *PDK4* encodes an enzyme critical for inhibiting the pyruvate dehydrogenase (PDH) complex. This inhibition halts the conversion of pyruvate into acetyl-CoA, reducing glycolytic flux and promoting fatty acid oxidation over glucose oxidation. Fasting conditions have been shown to upregulate *PDK4* [57, 58], a shift supported by our bioinformatics analysis, which suggests a metabolic transition from glycogenolysis to lipolysis and gluconeogenesis. *PDK4* is potentially influenced by *PPARγ* and circulating free fatty acids [59] and may also enhance *PPARγ* expression [60], though its primary function is to downregulate the PDH complex. This metabolic shift is particularly evident in the synovial tissue of RA patients and corresponding animal models, where anaerobic glycolysis becomes more dominant [61, 62]. Inhibiting this pathway via 3-bromopyruvate has reduced inflammation in arthritis models [63, 64]. The relationship between *PDK4* expression and RA disease activity also depends on the metabolic environment, showing either a positive [65] or negative [66] correlation. In our study, the observed upregulation of *Pdk4* in response to IF suggests a normal physiological adaptation to optimize energy use in conditions of limited nutrients.

The most downregulated genes in our study included *MUPs*, lipocalins involved in pheromonal communication, whose production represents a significant metabolic investment for *Mus musculus*. In addition to their role in chemical communication, *MUPs* appear to perform metabolic functions, increasing energy expenditure, core body temperature, glucose tolerance, and insulin sensitivity in mice [67]. It has been demonstrated that dietary intake can influence *MUP* expression and modulate their secretion [68], which aligns with our findings.

Il33, *Bglap*, *Cd79*, and over ten genes from various immunoglobulin chains stand out among the downregulated genes involved in inflammatory pathways. IHC confirmed the reduction of IL-33 in the hind paw joints of IF-treated mice. Notably, *IL-33*, a novel member of the IL-1 family, plays a critical role in RA by regulating signaling in macrophages, mast cells, granulocytes, and other immune cells. This marker correlates with rheumatoid factor, anti-cyclic citrullinated peptide antibodies, anti-mutant citrullinated vimentin, and IL-18 and has been proposed as a potential therapeutic target for RA [69]. Furthermore, *IL-33* is influenced by IF in the context of diabetes and obesity [70]. These findings suggest that IF may exert its anti-inflammatory effect in our model by downregulating *IL-33*, although further research is required to confirm this hypothesis.

The heat maps of diseases and biofunctions showed the anti-inflammatory effect of IF in CIA, where increased expression of genes related to lipid and carbohydrate metabolism, molecular transport, and small molecule biochemistry was observed. Consistent with this, the heat map also showed a reduction in metabolic diseases, cancer, and dysfunctions in endocrine, gastrointestinal, and reproductive systems due to IF. These results align with recent evidence suggesting that IF is a promising dietary intervention for autoimmune [17], chronic [71], gastrointestinal [72], and cardiovascular diseases [73], as well as for type 1 and type 2 diabetes [74], aging [75], and cancer [76].

Our transcriptome analysis revealed that non-coding RNAs were among the most differentially expressed, indicating a significant influence of transcriptional regulators in mediating the anti-inflammatory effect of IF. Several miRNAs altered by IF have previously been shown to regulate inflammatory processes and joint metabolism, particularly in the pathogenesis of OA, including *miR-15b* [39, 40], *mirR-103* [41, 42], *miR-302a* [43], and *miR5624* [44]. In addition to miRNAs, our study identified the deregulation of other non-coding RNAs, such as lncRNAs, implicated in genetic modulation due to IF.

One mechanism by which IF exerts its effects is modifying the gut microbiome [13, 15, 77]. In RA, dysbiosis of the gut microbiota and its metabolites is closely linked to disease progression via the inflammatory gut-joint axis

[78]. While the exact mechanisms are not fully understood, it is known that immunomodulatory cells in the proximal intestine act as intermediaries, allowing the microbiota to influence the onset and progression of RA. The gut microbiota composition differs significantly from healthy controls in early disease stages. The microbiota produces several compounds, such as enzymes, SCFAs, and metabolites, that maintain gut homeostasis; an imbalance in their production leads to inflammation. Proinflammatory compounds produced by bacteria in dysbiosis can leak into the bloodstream through a compromised intestinal barrier, contributing to systemic inflammation that eventually affects the joints [79, 80]. Restoring a healthy microbiome is currently considered a potential therapeutic strategy for RA [81, 82].

Given the strong connection between gut microbiome dysbiosis and RA and the role of IF in correcting this dysbiosis, our metagenomic sequencing allowed us to investigate how microbiome modification contributes to the observed anti-inflammatory effects in joints. Our results indicate that IF increases bacteria abundance and diversity, which becomes relevant considering that gut microbiota abundance and diversity decrease in RA, contributing to the disease's inflammatory processes [83]. Furthermore, in DBA/1 mice with CIA, bacterial abundance and diversity are significantly reduced, with a notable decrease in the prevalence of Bacteroides compared to naïve DBA/1 mice [84]. Our findings indicate that IF enhances the abundance of the order Bacteroidales, recognized for their ability to ferment dietary fiber, produce SCFA, especially acetate and propionate [85], and exert an anti-inflammatory effect.

Similarly, our results indicate a significant increase in the abundance of the Clostridia class, specifically within the Oscillospirales order and Ruminococcaceae family. These groups are well-known for their capacity to produce butyrate, an SCFA crucial in reducing inflammation and modulating immune responses [86]. Restoring gut microbiota through enhancing Ruminococcaceae has been proposed as a therapeutic strategy for inflammatory diseases, as it can increase SCFA production and mitigate systemic inflammation [87]. Our findings are further consistent with previous studies demonstrating the ability of intermittent fasting to increase SCFA-producing bacteria, including Bacteroidales and Ruminococcaceae [88, 89]. Taking our results together, we can suggest that microbiome modulation is one of the mechanisms by which IF exerted its anti-inflammatory effect in our arthritis model.

The overall findings from our analyses suggest that IF has anti-inflammatory potential and could serve as a strategy to enhance therapeutic responses in patients with RA. However, we acknowledge some limitations of our study. As a preclinical investigation, this research is the first to detail several molecular mechanisms modified by IF in arthritis; nonetheless, these findings require confirmation in patients with the disease. Additionally, the transcriptomic profile does not encompass all cellular events. While the reduction in inflammation was clinically and histologically validated, significant molecular aspects, including epigenetic regulatory processes, were not addressed. Thus, further evaluations through epigenomics, proteomics, and functional assays are still necessary.

Conclusions

Since IF does not significantly influence the effects of pharmacological interventions, it could be considered an adjunctive alternative to improve response to current treatment. IF positively impacts various inflammatory conditions and is safe for most patients. Our study indicates a potential benefit attributed to the intervention of IF on key pathogenic processes in CIA, warranting further exploration in human patients with RA.

Abbreviations

ANOVA	Analysis of variance
BCR	B cell receptor
BGLAP	Bone gamma-carboxyglutamate protein
BSA	Bovine serum albumin
CD	Cluster of differentiation
cDNA	Complementary DNA
CEBPB	CCAAT enhancer binding protein beta
CIA	Collagen-induced arthritis
DAB	Diaminobenzidine
DADA	Divisive Amplicon Denoising Algorithm
DEG	Differentially expressed gen
EREG	Epiregulin
FC	Fold change
FOXO	Forkhead box protein
FR	False discovery rate
GEO	Gene Expression Omnibus
H&E	Hematoxylin and eosin
HIF	Hypoxia-inducible factor
IF	Intermittent fasting
Ig	Immunoglobulins
IHC	Immunohistochemistry
IL	Interleukin
IPA	Ingenuity Pathway Analysis
lncRNA	long non-coding RNA
miRNA	microRNA
MUP	Major Urinary Proteins
NCBI	National Center for Biotechnology Information
OA	Osteoarthritis
OD	Optical density
OTU	Operational taxonomic units
PBS	Phosphate Buffered Saline
PDK	Pyruvate dehydrogenase kinase
PERMANOVA	Permutational multivariate analysis of variance
PPAR	Peroxisome proliferator-activated receptor
QIIME	Quantitative Insights Into Microbial Ecology
RA	Rheumatoid Arthritis
RMA	Robust Multiarray Averaging
RNA	Ribonucleic acid
RPL	Ribosomal protein L
RQ	Relative quantification
RT-qPCR	Retro Transcription-quantitative Polymerase Chain Reaction
SD	Standard deviation
SLE	Systemic Lupus Erythematous
TCR	T cell receptor

Supplementary Information

The online version contains supplementary material available at https://doi.org/10.1186/s41927-024-00436-0.

Supplementary Material 1

Supplementary Material 2

Supplementary Material 3

Acknowledgements
Not applicable.

Author contributions
Conceptualization: SAG-CH, CP-T; Data curation: RC-M, MB, JSS-L, SAG-CH, CP-T; Formal analysis: RC-M, MB, JSS-L, SAG-CH, CP-T; Funding acquisition: CP-T, SAG-CH, LCH-G; Investigation: RC-M SAG-CH, ECH-B, LCH-G, CP-S, CEV-M, GV-O, CR-S, CP-T; Methodology: RC-M, SAG-CH, CP-T; Project administration: SAG-CH, CP-T; Resources: RC-M, ECH-B, LCH-G, CP-S, CR-S, CEV-M, SAG-CH, CP-T; Supervision: SAG-CH, CP-T; Validation: SAG-CH, MB, JSS-L; Visualization: RC-M, SAG-CH, MB; Writing original draft: RC-M, SAG-CH, CP-T; Writing review & editing: MB, JSS-L, GV-O, ECH-B, LCH-G, CP-S, CR-S, CEV-M.

Funding
Investigación y Biomedicina de Chihuahua, S.C, partially founded this investigation.

Data availability
The microarray dataset was registered in the Gene Expression Omnibus (GEO) of the National Center for Biotechnology Information (NCBI) database with the accession number GSE242986.The dataset generated from 16 S rRNA sequencing was deposited into NCBI, and it is available under BioProject PRJNA1107524.

Declarations

Ethics approval and consent to participate
This study complied with the Official Mexican Standard NOM-062-ZOO-1999, technical specifications for producing, caring for, and using laboratory animals. The Ethics Committee and Institutional Animal Care and Use Committee (IACUC) from the Faculty of Medicine and Biomedical Sciences of the Autonomous University of Chihuahua approved the research (ID number: CI-013-22).

Consent for publication
Not applicable.

Competing interests
The authors declare no competing interests.

Author informations
Not applicable.

Author details
[1]PABIOM Laboratory, Faculty of Medicine and Biomedical Sciences, Autonomous University of Chihuahua, Circuito Universitario Campus II, Chihuahua, CP 31125, Mexico
[2]Faculty of Dentistry, Autonomous University of Chihuahua, Chihuahua, Mexico
[3]Advanced Materials Research Center (CIMAV), S.C. Chihuahua, Mexico
[4]Faculty of Medicine and Biomedical Sciences, Autonomous University of Chihuahua, Chihuahua, Mexico
[5]Cellular and Molecular Immunology Group (INMUBO), School of Dentistry, Universidad El Bosque, Bogotá, Colombia

Received: 29 August 2024 / Accepted: 11 November 2024
Published online: 25 November 2024

References

1. Alivernini S, Firestein GS, McInnes IB. The pathogenesis of rheumatoid arthritis. Immunity. 2022;55:2255–70.
2. Buch MH, Eyre S, McGonagle D. Persistent inflammatory and non-inflammatory mechanisms in refractory rheumatoid arthritis. Nat Rev Rheumatol. 2021;17:17–33.
3. Langrish CL, Chen Y, Blumenschein WM, Mattson J, Basham B, Sedgwick JD, et al. IL-23 drives a pathogenic T cell population that induces autoimmune inflammation. J Exp Med. 2005;201:233–40.
4. Philippou E, Petersson SD, Rodomar C, Nikiphorou E. Rheumatoid arthritis and dietary interventions: systematic review of clinical trials. Nutr Rev. 2021;79:410–28.
5. Pelc M. The effects of Intermittent Fasting and a low-carbohydrate Diet on type 2 diabetes. Jaapa. 2023. https://doi.org/10.1097/01.jaa.0000923536.23229.d3.
6. Tang D, Tang Q, Huang W, Zhang Y, Tian Y, Fu X. Fasting: from physiology to Pathology. Adv Sci. 2023;10:2204487.
7. Asbath. Different types of intermittent fasting for Glucosa Index Control in diabetics: a systematic review. J Nurs Pract. 2024. https://doi.org/10.30994/jnp.v7i2.504.
8. Gu L, Fu R, Hong J, Ni H, Yu K, Lou H. Effects of Intermittent Fasting in Human compared to a Non-intervention Diet and caloric restriction: a Meta-analysis of Randomized controlled trials. Front Nutr. 2022. https://doi.org/10.3389/fnut.2022.871682.
9. Longo VD, Mattson MP. Fasting: Molecular mechanisms and clinical applications. Cell Metabol. 2014;19:181–92.
10. De Cabo R, Mattson MP. Effects of Intermittent Fasting on Health, Aging, and Disease. N Engl J Med. 2019;381:2541–51.
11. Albosta M, Bakke J. Intermittent fasting: is there a role in the treatment of diabetes? A review of the Literature and Guide for Primary Care Physicians. Clin Diabetes Endocrinol. 2021. https://doi.org/10.1186/s40842-020-00116-1.
12. Shabkhizan R, Haiaty S, Moslehian MS, Bazmani A, Sadeghsoltani F, Saghaei Bagheri H, et al. The beneficial and adverse effects of Autophagic response to caloric restriction and fasting. Adv Nutr. 2023;14:1211–25.
13. Liu Z, Dai X, Zhang H, Shi R, Hui Y, Jin X, et al. Gut microbiota mediates intermittent-fasting alleviation of diabetes-induced cognitive impairment. Nat Commun. 2020;11:855.
14. Kim YC, Guan K-L. mTOR: a pharmacologic target for autophagy regulation. J Clin Invest. 2015;125:25–32.
15. Pérez-Gerdel T, Camargo M, Alvarado M, Ramírez JD. Impact of intermittent fasting on the gut microbiota: a systematic review. Adv Biology. 2023;7:2200337.
16. Sharma P, Brown S, Sokoya EM. Re-evaluation of dietary interventions in rheumatoid arthritis: can we improve patient conversations around food choices? Rheumatol Int. 2024;44:1409–19.
17. Barati M, Ghahremani A, Namdar Ahmadabad H. Intermittent fasting: a promising dietary intervention for autoimmune diseases. Autoimmun Rev. 2023;22:103408.
18. Khanna S, Jaiswal KS, Gupta B. Managing rheumatoid arthritis with dietary interventions. Front Nutr. 2017;4:52.
19. Ranjbar M, Shab-Bidar S, Rostamian A, Mohammadi H, Djafarian K. The effects of intermittent fasting diet on quality of life, clinical symptoms, inflammation, and oxidative stress in overweight and obese postmenopausal women with rheumatoid arthritis: study protocol of a randomized controlled trial. Trials. 2024;25:168.
20. Ben Nessib D, Maatallah K, Ferjani H, Triki W, Kaffel D, Hamdi W. Sustainable positive effects of Ramadan intermittent fasting in rheumatoid arthritis. Clin Rheumatol. 2022;41:399–403.
21. Ciaffi J, Mitselman D, Mancarella L, Brusi V, Lisi L, Ruscitti P, et al. The Effect of Ketogenic Diet on Inflammatory Arthritis and Cardiovascular Health in Rheumatic conditions: a Mini Review. Front Med. 2021;8:792846.
22. Grajower MM, Horne BD. Clinical management of intermittent fasting in patients with diabetes Mellitus. Nutrients. 2019;11:873.
23. Vasim I, Majeed CN, DeBoer MD. Intermittent Fasting Metabolic Health Nutrients. 2022;14:631.
24. Corley BT, Carroll RW, Hall RM, Weatherall M, Parry-Strong A, Krebs JD. Intermittent fasting in type 2 diabetes mellitus and the risk of hypoglycaemia: a randomized controlled trial. Diabet Med. 2018;35:588–94.
25. Chaudhury A, Duvoor C, Reddy Dendi VS, Kraleti S, Chada A, Ravilla R et al. Clinical review of antidiabetic drugs: implications for type 2 diabetes Mellitus Management. Front Endocrinol. 2017;8.

26. Carter S, Clifton PM, Keogh JB. Effect of intermittent compared with continuous energy restricted Diet on Glycemic Control in patients with type 2 diabetes: a Randomized Noninferiority Trial. JAMA Netw Open. 2018;1:e180756.
27. Kalam F, Akasheh RT, Cienfuegos S, Ankireddy A, Gabel K, Ezpeleta M, et al. Effect of time-restricted eating on sex hormone levels in premenopausal and postmenopausal females. Obesity. 2023;31:57–62.
28. Wilson R, Deasy W, Stathis C, Hayes A, Cooke M. Intermittent fasting with or without Exercise prevents Weight Gain and improves lipids in Diet-Induced obese mice. Nutrients. 2018;10:346.
29. Wei S, Zhao J, Bai M, Li C, Zhang L, Chen Y. Comparison of glycemic improvement between intermittent calorie restriction and continuous calorie restriction in diabetic mice. Nutr Metab (Lond). 2019;16:60.
30. Li D, Onodera S, Deng S, Alnujaydi B, Yu Q, Zhou J. Alternate-day fasting ameliorates newly established Sjögren's syndrome-like Sialadenitis in non-obese Diabetic mice. IJMS. 2022;23:13791.
31. Cui J, Lee S, Sun Y, Zhang C, Hill MA, Li Y, et al. Alternate day fasting improves endothelial function in type 2 Diabetic mice: role of adipose-derived hormones. Front Cardiovasc Med. 2022;9:925080.
32. Miyoshi M, Liu S. Collagen-Induced Arthritis models. In: Liu S, editor. Rheumatoid arthritis. New York, NY: Springer US; 2024. pp. 3–7.
33. Zhang X, Zou Q, Zhao B, Zhang J, Zhao W, Li Y, et al. Effects of alternate-day fasting, time-restricted fasting and intermittent energy restriction DSS-induced on colitis and behavioral disorders. Redox Biol. 2020;32:101535.
34. Brand DD, Latham KA, Rosloniec EF. Collagen-induced arthritis. Nat Protoc. 2007;2:1269–75.
35. Benjamini Y, Hochberg Y. Controlling the false Discovery rate: a practical and powerful Approach to multiple testing. J Roy Stat Soc: Ser B (Methodol). 1995;57:289–300.
36. Quiñonez-Flores CM, López-Loeza SM, Pacheco-Tena C, Muñoz-Morales PM, Acosta-Jiménez S, González-Chávez SA. Stability of housekeeping genes in inflamed joints of spontaneous and collagen-induced arthritis in DBA/1 mice. Inflamm Res. 2021;70:619–32.
37. Bolyen E, Rideout JR, Dillon MR, Bokulich NA, Abnet CC, Al-Ghalith GA, et al. Reproducible, interactive, scalable and extensible microbiome data science using QIIME 2. Nat Biotechnol. 2019;37:852–7.
38. Chong J, Liu P, Zhou G, Xia J. Using MicrobiomeAnalyst for comprehensive statistical, functional, and meta-analysis of microbiome data. Nat Protoc. 2020;15:799–821.
39. Liu T, Li G. miR-15b-5p transcription mediated by CREB1 protects against inflammation and apoptosis in Parkinson disease models by inhibiting AXIN2 and activating Wnt/β-catenin. J Neuropathology Experimental Neurol. 2023;82:995–1009.
40. Yu X-M, Meng H-Y, Yuan X-L, Wang Y, Guo Q-Y, Peng J, et al. MicroRNAs' involvement in Osteoarthritis and the prospects for treatments. Evidence-Based Complement Altern Med. 2015;2015:1–13.
41. Chen J, Wu X. MicroRNA-103 contributes to osteoarthritis development by targeting Sox6. Biomed Pharmacother. 2019;118:109186.
42. Renman E, Brink M, Ärlestig L, Rantapää-Dahlqvist S, Lejon K. Dysregulated microRNA expression in rheumatoid arthritis families—a comparison between rheumatoid arthritis patients, their first-degree relatives, and healthy controls. Clin Rheumatol. 2021;40:2387–94.
43. Zhang Q, Fang X, Zhao W, Liang Q. The transcriptional coactivator YAP1 is overexpressed in osteoarthritis and promotes its progression by interacting with Beclin-1. Gene. 2019;689:210–9.
44. Kwak YH, Kwak D-K, Kim NY, Kim YJ, Lim JS, Yoo J-H. Significant changes in synovial fluid microRNAs after high tibial osteotomy in medial compartmental knee osteoarthritis: identification of potential prognostic biomarkers. PLoS ONE. 2020;15:e0227596.
45. Dai S, Wei J, Zhang H, Luo P, Yang Y, Jiang X, et al. Intermittent fasting reduces neuroinflammation in intracerebral hemorrhage through the Sirt3/Nrf2/HO-1 pathway. J Neuroinflammation. 2022;19:122.
46. Wang C, Zhang X, Luo L, Luo Y, Yang X, Ding X, et al. Adipocyte-derived PGE2 is required for intermittent fasting–induced Treg proliferation and improvement of insulin sensitivity. JCI Insight. 2022;7:e153755.
47. Tateiwa. Yoshikawa, Kaito. Cartilage and Bone Destruction in Arthritis: Pathogenesis and Treatment Strategy: A literature review. Cells. 2019;8:818.
48. Ben Achour W, Bouaziz M, Mechri M, Zouari B, Bahlous A, Abdelmoula L, et al. A cross sectional study of bone and cartilage biomarkers: correlation with structural damage in rheumatoid arthritis. Libyan J Med. 2018;13:1512330.
49. Cai P, Lu Z, Jiang T, Wang Z, Yang Y, Zheng L, et al. Syndecan-4 involves in the pathogenesis of rheumatoid arthritis by regulating the inflammatory response and apoptosis of fibroblast-like synoviocytes. J Cell Physiol. 2020;235:1746–58.
50. Tyagi N, Mehla K, Gupta D. Deciphering novel common gene signatures for rheumatoid arthritis and systemic lupus erythematosus by integrative analysis of transcriptomic profiles. PLoS ONE. 2023;18:e0281637.
51. Zhou J, Li H, Xia X, Herrera A, Pollock N, Reebye V, et al. Anti-inflammatory activity of MTL-CEBPA, a small activating RNA drug, in LPS-Stimulated monocytes and Humanized mice. Mol Ther. 2019;27:999–1016.
52. Garg NK, Tyagi RK, Singh B, Sharma G, Nirbhavane P, Kushwah V, et al. Nanostructured lipid carrier mediates effective delivery of methotrexate to induce apoptosis of rheumatoid arthritis via NF-κB and FOXO1. Int J Pharm. 2016;499:301–20.
53. Hong Z, Tie Q, Zhang L. Targeted inhibition of the GRK2/HIF-1α pathway is an effective strategy to alleviate synovial hypoxia and inflammation. Int Immunopharmacol. 2022;113:109271.
54. Li X, Yin S, Li H, Yang Y, Chen X, Song B, et al. PPAR-γ alleviates the inflammatory response in TNF-α-induced fibroblast-like synoviocytes by binding to p53 in rheumatoid arthritis. Acta Pharmacol Sin. 2023;44:454–64.
55. Yusta B, Holland D, Koehler JA, Maziarz M, Estall JL, Higgins R, et al. ErbB signaling is required for the proliferative actions of GLP-2 in the murine gut. Gastroenterology. 2009;137:986–96.
56. de Heuvel E, Wallace L, Sharkey KA, Sigalet DL. Glucagon-like peptide 2 induces vasoactive intestinal polypeptide expression in enteric neurons via phophatidylinositol 3-kinase-γ signaling. Am J Physiol Endocrinol Metab. 2012;303:E994–1005.
57. Araki M, Nozaki Y, Motojima K. [Transcriptional regulation of metabolic switching PDK4 gene under various physiological conditions]. Yakugaku Zasshi. 2007;127:153–62.
58. Gudiksen A, Pilegaard H. PGC-1α and fasting-induced PDH regulation in mouse skeletal muscle. Physiol Rep. 2017;5:e13222.
59. Yamaguchi S, Moseley AC, Almeda-Valdes P, Stromsdorfer KL, Franczyk MP, Okunade AL, et al. Diurnal variation in PDK4 expression is Associated with plasma free fatty acid availability in people. J Clin Endocrinol Metab. 2018;103:1068–76.
60. Li Z, Xie L, Zeng H, Wu Y. PDK4 inhibits osteoarthritis progression by activating the PPAR pathway. J Orthop Surg Res. 2024;19:109.
61. Henderson B, Bitensky L, Chayen J. Glycolytic activity in human synovial lining cells in rheumatoid arthritis. Ann Rheum Dis. 1979;38:63–7.
62. Ciurtin C, Cojocaru VM, Miron IM, Preda F, Milicescu M, Bojincă M, et al. Correlation between different components of synovial fluid and pathogenesis of rheumatic diseases. Rom J Intern Med. 2006;44:171–81.
63. Okano T, Saegusa J, Nishimura K, Takahashi S, Sendo S, Ueda Y, et al. 3-bromopyruvate ameliorate autoimmune arthritis by modulating Th17/Treg cell differentiation and suppressing dendritic cell activation. Sci Rep. 2017;7:42412.
64. Panneton V, Bagherzadeh Yazdchi S, Witalis M, Chang J, Suh W-K. ICOS Signaling Controls Induction and maintenance of Collagen-Induced Arthritis. J Immunol. 2018;200:3067–76.
65. W Z BL et al. N X, L Z, Z Z, Z R,. lncRNA GAS5 suppresses rheumatoid arthritis by inhibiting miR-361-5p and increasing PDK4. Biochemical and biophysical research communications. 2021;583.
66. Liu D, Fang Y, Rao Y, Tan W, Zhou W, Wu X, et al. Synovial fibroblast-derived exosomal microRNA-106b suppresses chondrocyte proliferation and migration in rheumatoid arthritis via down-regulation of PDK4. J Mol Med (Berl). 2020;98:409–23.
67. Hui X, Zhu W, Wang Y, Lam KSL, Zhang J, Wu D, et al. Major urinary Protein-1 increases Energy expenditure and improves glucose intolerance through enhancing mitochondrial function in skeletal muscle of Diabetic mice. J Biol Chem. 2009;284:14050–7.
68. Giller K, Huebbe P, Doering F, Pallauf K, Rimbach G. Major urinary protein 5, a scent communication protein, is regulated by dietary restriction and subsequent re-feeding in mice. Proc R Soc B. 2013;280:20130101.
69. Ouyang T, Song L, Fang H, Tan J, Zheng Y, Yi J. Potential mechanistic roles of Interleukin-33 in rheumatoid arthritis. Int Immunopharmacol. 2023;123:110770.
70. Miller AM, Asquith DL, Hueber AJ, Anderson LA, Holmes WM, McKenzie AN, et al. Interleukin-33 induces protective effects in adipose tissue inflammation during obesity in mice. Circ Res. 2010;107:650–8.
71. Cheng W-Y, Desmet L, Depoortere I. Time-restricted eating for chronodisruption-related chronic diseases. Acta Physiol (Oxf). 2023;:e14027.

72. Tibi S, Ahmed S, Nizam Y, Aldoghmi M, Moosa A, Bourenane K, et al. Implications of Ramadan Fasting in the setting of gastrointestinal disorders. Cureus. 2023;15:e36972.
73. Diab A, Dastmalchi LN, Gulati M, Michos ED. A heart-healthy Diet for Cardiovascular Disease Prevention: where are we now? Vasc Health Risk Manag. 2023;19:237–53.
74. Herz D, Haupt S, Zimmer RT, Wachsmuth NB, Schierbauer J, Zimmermann P, et al. Efficacy of fasting in type 1 and type 2 diabetes Mellitus: a narrative review. Nutrients. 2023;15:3525.
75. Chaudhary MR, Chaudhary S, Sharma Y, Singh TA, Mishra AK, Sharma S, et al. Aging, oxidative stress and degenerative diseases: mechanisms, complications and emerging therapeutic strategies. Biogerontology. 2023;24:609–62.
76. Anemoulis M, Vlastos A, Kachtsidis V, Karras SN. Intermittent fasting in breast Cancer: a systematic review and critical update of available studies. Nutrients. 2023;15:532.
77. Saglam D, Colak GA, Sahin E, Ekren BY, Sezerman U, Bas M. Effects of Ramadan intermittent fasting on gut microbiome: is the diet key? Front Microbiol. 2023;14:1203205.
78. Zaiss MM, Joyce Wu H-J, Mauro D, Schett G, Ciccia F. The gut–joint axis in rheumatoid arthritis. Nat Rev Rheumatol. 2021;17:224–37.
79. Longo UG, Lalli A, Bandini B, De Sire R, Angeletti S, Lustig S, et al. Role of the gut microbiota in Osteoarthritis, Rheumatoid Arthritis, and Spondylarthritis: an update on the gut–joint Axis. IJMS. 2024;25:3242.
80. Mahroum N, Seida R, Shoenfeld Y. Triggers and regulation: the gut microbiome in rheumatoid arthritis. Expert Rev Clin Immunol. 2023;19:1449–56.
81. Williams KL, Enslow R, Suresh S, Beaton C, Hodge M, Brooks AE. Using the Microbiome as a Regenerative Medicine Strategy for Autoimmune diseases. Biomedicines. 2023;11:1582.
82. Zhao T, Wei Y, Zhu Y, Xie Z, Hai Q, Li Z, et al. Gut microbiota and rheumatoid arthritis: from pathogenesis to novel therapeutic opportunities. Front Immunol. 2022;13:1007165.
83. Wang Y, Wei J, Zhang W, Doherty M, Zhang Y, Xie H, et al. Gut dysbiosis in rheumatic diseases: a systematic review and meta-analysis of 92 observational studies. eBioMedicine. 2022;80:104055.
84. Rogier R, Evans-Marin H, Manasson J, Van Der Kraan PM, Walgreen B, Helsen MM, et al. Alteration of the intestinal microbiome characterizes preclinical inflammatory arthritis in mice and its modulation attenuates established arthritis. Sci Rep. 2017;7:15613.
85. Rios-Covian D, Salazar N, Gueimonde M, De Los Reyes-Gavilan CG. Shaping the metabolism of Intestinal Bacteroides Population through Diet to Improve Human Health. Front Microbiol. 2017;8.
86. Kim Y-J, Jung D-H, Park C-S. Important roles of Ruminococcaceae in the human intestine for resistant starch utilization. Food Sci Biotechnol. 2024;33:2009–19.
87. Zhao H, Zhou Y, Xu J, Zhang Y, Wang H, Zhao C, et al. Short-chain fatty acid-producing bacterial strains attenuate experimental ulcerative colitis by promoting M2 macrophage polarization via JAK/STAT3/FOXO3 axis inactivation. J Transl Med. 2024;22:369.
88. Angoorani P, Ejtahed H-S, Hasani-Ranjbar S, Siadat SD, Soroush AR, Larijani B. Gut microbiota modulation as a possible mediating mechanism for fasting-induced alleviation of metabolic complications: a systematic review. Nutr Metab (Lond). 2021;18:105.
89. Su J, Li F, Wang Y, Su Y, Verhaar A, Ma Z, et al. Investigating Ramadan like Fasting effects on the gut microbiome in BALB/c mice. Front Nutr. 2022;9:832757.

Publisher's note